Amplification and stabilization of large-amplitude propagating spin waves by parametric pumping

Roman Verba, Mario Carpentieri, Giovanni Finocchio, Vasil Tiberkevich, and Andrei Slavin

Citation: Appl. Phys. Lett. **112**, 042402 (2018);
View online: https://doi.org/10.1063/1.5019357
View Table of Contents: http://aip.scitation.org/toc/apl/112/4
Published by the American Institute of Physics

Amplification and stabilization of large-amplitude propagating spin waves by parametric pumping

Roman Verba,[1,a)] Mario Carpentieri,[2] Giovanni Finocchio,[3] Vasil Tiberkevich,[4] and Andrei Slavin[4]
[1]*Institute of Magnetism, Kyiv 03680, Ukraine*
[2]*Department of Electrical and Information Engineering, Politecnico di Bari, I-70125 Bari, Italy*
[3]*Department of Electronic Engineering, Industrial Chemistry and Engineering, University of Messina, I-98166 Messina, Italy*
[4]*Department of Physics, Oakland University, Rochester, Michigan 48309, USA*

(Received 13 December 2017; accepted 10 January 2018; published online 22 January 2018)

The interaction of a localized parametric pumping with spin waves of different amplitudes, propagating in a ferromagnetic nanowire, is studied analytically and by micromagnetic simulations. It is shown that parametric amplification of spin waves by localized pumping becomes less efficient with an increase in the spin wave amplitude due to the influence of nonlinear 4-magnon processes. In a certain range of spin wave amplitudes, the parametric amplifier acts as a stabilizer of the spin wave amplitude, as its action significantly reduces the spread of the spin wave amplitude in the vicinity of a certain mean value. The stabilization effect becomes more pronounced for higher pumping strength and larger relative lengths of the pumping localization region, compared to the spin wave mean free path. In contrast, the use of relatively short pumping localization regions allows one to efficiently amplify large-amplitude nonlinear spin waves. *Published by AIP Publishing.*
https://doi.org/10.1063/1.5019357

Recent experimental and theoretical investigations[1–6] have shown that spin waves (SWs) in magnetic micro- and nano-structures can be successfully used in microwave signal processing. These SWs have high frequencies (up to tens of gigahertz) and short wavelengths (down to several nanometers), and their dispersion characteristic can be effectively controlled by the structure sizes, as well as by the magnitude and direction of the applied bias magnetic field. The discovery of the interfacial Dzyaloshinskii-Moriya interaction, which can lead to SW nonreciprocity at the nanoscale,[7–9] and studies of the effect of voltage-controlled magnetic anisotropy (VCMA),[10,11] which enables low-loss excitation and manipulation of SWs using electric fields,[12–15] create additional advantages for signal processing by means of microwave SWs.

To build a practical SW-based signal processing circuit, one should find a way to perform several basic operations with SWs, such as SW excitation and reception, controllable modification of the SW amplitude and phase, and logic operations. One of such necessary basic operations is the amplification of a propagating SW, which is required to compensate the SW propagation losses as well as the SW processing losses. Another basic operation that could be critically important in signal processing is the stabilization of the SW amplitude, i.e., the operation that could make the amplitude of an output SW almost the same in a certain range of input SW amplitudes. The operation of the amplitude stabilization is especially important in the SW-based signal processing circuits where phase modulation is used to code the transmitted information and the SW interference is used to perform signal-processing operations.[2,5,16,17] Indeed, the result of interference of two or more SWs is sensitive to their phases only if the SW amplitudes are almost the same. Otherwise, the result of the SW interference may substantially depend on the relative amplitudes of input SWs, while the SW phase information may be lost completely.

In this work, we will show that both amplification and amplitude stabilization of a SW-coded signal can be realized by localized parametric pumping—i.e., by the interaction of a propagating SW with a localized magnetic field (external or effective) of approximately double SW frequency. The parametric pumping is a well-known experimental method for the frequency-selective amplification of *linear* (small amplitude) propagating SWs.[18–22] However, in ferromagnetic nanowires it is possible and, in order to increase the signal-to-noise ratio, often desirable to have relatively large-amplitude SWs.[23] Below, we will specifically study the influence of the amplitude of a propagating SW on the process of its parametric interaction with pumping and will clarify when the pumping could be used for effective SW amplification and when this pumping can work as a SW amplitude stabilizer.

A sketch of the studied system is shown in Fig. 1. It is a ferromagnetic nanowire of width w_y and thickness h, having

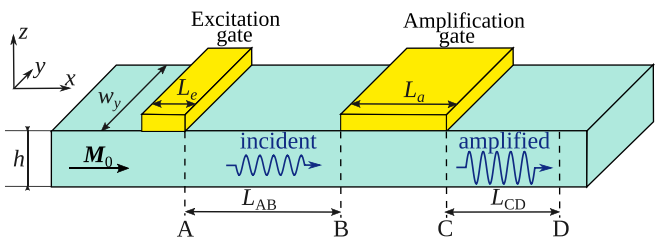

FIG. 1. A sketch of the parametric amplifier showing regions where excitation and amplification of the propagating spin waves take place. The reference points A-D used in the micromagnetic simulations are also shown.

a)Author to whom correspondence should be addressed: verrv@ukr.net

the in-plane static magnetization due to the nanowire shape anisotropy. We considered the VCMA-based parametric pumping which is realized by variation of the perpendicular anisotropy at a ferromagnetic—dielectric interface at the microwave voltage applied across the interface. Our previous work[24] showed that in this geometry, microwave anisotropy couples parametrically to the propagating SWs, and it can be used for the efficient excitation or/and amplification of SWs. Note, also, that all the results presented below are rather general and could be used in a case when pumping is provided by other means (e.g., by a localized microwave magnetic field) and when other nanowire geometry and direction of the static magnetization are used.

The process of parametric pumping of small-amplitude SWs has been studied in detail in Refs. 18 and 25 and references therein. The parametric pumping, which in our case is created by microwave-frequency modulation of perpendicular magnetic anisotropy, couples with two propagating SWs having wave vectors k and k' and can pump energy into these waves. In particular, if a propagating SW having wave vector k and frequency ω_k passes through the region of pumping localization, the parametric interaction results in the partial compensation of the propagation losses or in the amplification of this SW and in the simultaneous creation of an idler SW having the wave vector k' and frequency $\omega_{k'}$. The parametric interaction is the most efficient if $k' \approx -k$ and the pumping frequency $\omega_p = \omega_k + \omega_{k'}$, i.e., if the conservation laws for the linear momentum and energy are fulfilled. In the simplest case of a *reciprocal* SW spectrum $\omega_k = \omega_{-k}$ leading to the parametric resonance condition $\omega_p = 2\omega_k$, the frequency of parametric pumping should be twice larger than the frequency of the propagating SW. In this case, the amplification rate (the ratio of the signal SW amplitude after and before the interaction with pumping) is equal to[20]

$$K = \left[\cos \kappa L_a + \frac{\Gamma_k}{v\kappa} \sin \kappa L_a\right]^{-1}, \quad \kappa = \frac{\sqrt{|Vb_p|^2 - \Gamma_k^2}}{v}, \quad (1)$$

and is determined by the SW group velocity v, damping rate Γ_k, length of the pumping localization region L_a, and the efficiency of the parametric interaction $V = V_{kk}$, which in our case is equal to $V_{kk} = \gamma m_{k,z}/(4m_{k,y})$, where $m_{k,y}$ and $m_{k,z}$ are the dynamic magnetization components of SW.[24] The amplification rate increases with the pumping strength b_p (effective magnetic field of the pumping) and, at a certain value of $b_p = b_{\text{th}}$, becomes infinite, $K \to \infty$, meaning that two counter-propagating SWs are excited spontaneously by parametric pumping. Of course, for the purpose of the SW amplification, the pumping should be always below this critical value, $b_p < b_{\text{th}}$.

When the condition of the parametric resonance $\omega_p = 2\omega_k$ is not satisfied exactly, the amplification rate decreases rapidly at the frequency scale proportional to the SW damping rate Γ_k, resulting in the amplification that is strongly frequency-selective. Equation (1) uses the assumption of the *adiabatic* pumping, meaning that the pumping localization length L_a is larger than the SW wavelength (strictly speaking, if $|\text{sinc}[kL_a]| \ll 1$). Otherwise, the amplification rate becomes dependent on the SW phase[26,27] that is undesirable in a general case (but could have its own specific applications[28]).

Equation (1) is valid for moderate amplification rates K, when the amplitudes of both incident and amplified SWs, as well as the amplitude of the idler SW, are sufficiently small to neglect the nonlinear SW interaction.

To study effects of nonlinear interaction on the parametric amplification of SW, we, first of all, performed micromagnetic simulations using the GPMagnet solver.[29,30] In the simulations, the SWs were excited linearly by microwave magnetic field $\boldsymbol{b} = b_y(t)\boldsymbol{e}_y$ applied at the excitation gate of the length $L_e = 30$ nm. The excitation frequency was 8.23 GHz, which corresponds to the SW wavelength of 100 nm. The microwave parametric pumping in the form of a perpendicular anisotropy $\Delta K_\perp = b_p M_s \cos[\omega_p t]$ modulated with the frequency $\omega_p/(2\pi) = 16.46$ GHz was applied at the amplification gate of the length $L_a = 500$ nm, separated from the excitation gate by the distance of $L_{\text{AB}} = 400$ nm. The transmission characteristic of the amplifier defined as the ratio of the SW amplitude at the amplification gate output (point C) to the SW amplitude at the amplification gate input (point B) was calculated for different magnitudes of the pumping strength (points B and C are shown in Fig. 1).

To avoid the incorrect determination of the SW amplitude due to the presence of the idler wave, the amplitude of the incident SW was obtained at a given excitation field and zero pumping, while the amplitude of the output SW at $x = x_C$ was retrieved from the amplitude at point D (separated from point C by the distance $L_{\text{CD}} = 400$ nm), where the idler wave is definitely absent, provided that the propagation losses are known. The following material parameters of the Fe/MgO structure (common for VCMA experiments) were used: saturation magnetization $\mu_0 M_s = 2.1$ T, exchange length $\lambda_{\text{ex}} = 3.4$ nm, surface perpendicular anisotropy energy $K_s = 1.36$ mJ/m^2, and effective Gilbert damping (including non-uniform broadening for a given SW frequency) $\alpha_G = 0.02$. The nanowire thickness was set to $h = 1$ nm and width $w = 20$ nm, and the bias magnetic field was absent. For such a width of a nanowire, all the SW modes, except the one that is uniform across the nanowire width, have the frequencies that are much higher than the studied one and, therefore, can be disregarded.

The simulated transmission characteristics calculated at the different values of the pumping strength are shown in Fig. 2. For the chosen parameters, the threshold of parametric excitation is equal to $b_p = 64$ mT, corresponding to the pumping electric field of 0.53 V/nm in the VCMA Fe/MgO structure. As one can see, in the interval of sufficiently small SW amplitudes, the transmission characteristics are linear, demonstrating that the amplification rate K is constant and is determined solely by the pumping amplitude. Then, the transmission characteristics demonstrate saturation, which corresponds to the decrease in the amplification rate. The saturation appears at different amplitudes of the incident SW for different magnitudes of the pumping strength: for a smaller pumping, the linear amplification regime is realized in a wider range of incident SW amplitudes. With a further increase in the incident SW amplitude, the parametric amplification becomes less and less efficient, and, finally, the output SW signal becomes almost insensitive to the presence of the parametric pumping (see below). If the pumping is switched off, SW decays at the pumping length with the rate $K = \exp[-L_a/l_{\text{fp}}]$, where $l_{\text{fp}} = v/\Gamma_k$ is the SW mean free

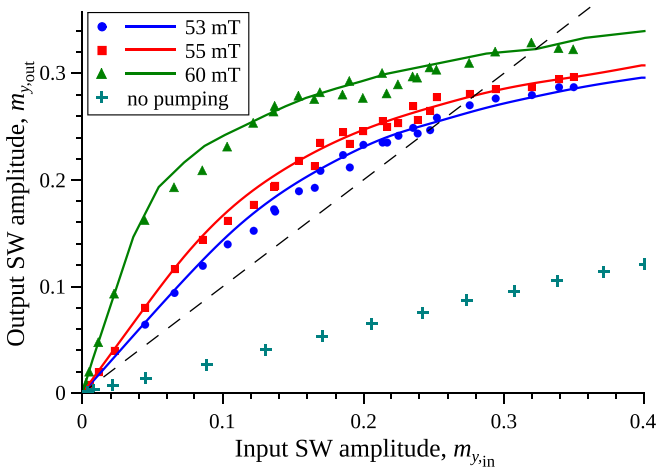

FIG. 2. Transmission characteristics of the parametric amplifier: symbols—micromagnetic simulations and lines—analytical model. The dashed line corresponds to the amplification rate $K = 1$ ($m_{y,out} = m_{y,in}$). The SW amplitudes are shown as a dimensionless dynamic magnetization component $m_y = M_y/M_s$.

path; for the studied case, $l_{fp} \approx 440$ nm and is almost independent of the SW amplitude within the studied range (Fig. 2).

Figure 2 illustrates, also, another interesting feature of the nonlinear parametric amplification. It can be seen that at a certain incident SW amplitude m_0, which depends on the pumping strength, the amplification rate is equal to $K = 1$, which corresponds to the situation when the amplitudes of the incident and the output SWs are equal. Note that the derivative of the transmission characteristics dm_{out}/dm_{in} at this point is less than 1. Then, if the incident SW near this point has an average amplitude m_0 with a certain amplitude spread Δm_{in}, $m_{in} = m_0 + \Delta m_{in}$, the output SW will also have the same mean amplitude m_0, but a smaller amplitude spread: $m_{out} = m_0 + \Delta m_{out}$, where $\Delta m_{out} = \Delta m_{in}$ $(dm_{out}/dm_{in}) < \Delta m_{in}$. Consequently, the parametric amplifier in this regime can be used for the stabilization of the output SW amplitude, which is a necessary operation for the processing of SW signals with phase modulation.

To give a further insight into the nonlinear parametric amplification process, we consider SW dynamics within a simplified analytical model. We use the so-called Bloembergen system of equations (see e.g., Ref. 26) which describes the evolution of envelope amplitudes of SW a_1 (signal wave) and a_2 (idler wave), which are related to the real magnetization by the equation $(M_y)_{1,2} = CM_s a_{1,2}(t,x)$ $\exp[i(\pm kx - \omega_k t)]$, where the coefficient C is dependent on the SW vector structure.[23,26] Then, the system of the Bloembergen equations can be written as

$$\left(\frac{\partial}{\partial t} + v\frac{\partial}{\partial x} + \Gamma\right)a_1 = -iVb_p(x)a_2^* - i(T|a_1|^2 + 2S|a_2|^2)a_1. \tag{2}$$

The second equation for the envelope amplitude a_2 can be obtained by the index replacement $1 \leftrightarrow 2$ and the change $v \to -v$. This system includes the effects of the SW propagation, damping, and interaction with pumping. The solution of Eq. (2) in the linear approximation ($T = S = 0$) with natural boundary conditions $a_1(x_B) = a_0$, $a_2(x_C) = 0$ gives the amplification rate Eq. (1).

In Eq. (2), we also include two nonlinear terms. The first one describes the nonlinear SW frequency shift $\omega = \omega_0 + T|c_k|^2$ (c_k is the SW amplitude), which is a result of 4-wave interaction of a SW with itself (corresponding Hamiltonian $\mathcal{H} = (1/2)\sum_k T_k|c_k|^4$). The second term describes the 4-wave interaction of the SW pairs with opposite wave vectors k and $-k$ (signal and idler SWs in our case), which is described by the Hamiltonian $\mathcal{H} = \sum_k S_k|c_k|^2|c_{-k}|^2$. The S-term is known to be often the most important nonlinear term for the processes of parametric wave interaction, as it is responsible for the deviation of the phase relation between the SWs and the parametric pumping from the optimum, and, consequently, in a less efficient energy transfer from the pumping to the SWs.[18] The coefficients $T = T_k$ and $S = S_k$ can be calculated using the formalism presented in Ref. 31 (also see Ref. 23).

The general analytical solution of Eq. (2) is not known, and before solving it numerically, it is useful to make one additional transformation of this equation. If one introduces new variables $a_1 = \tilde{a}_1 \exp[-i(T/v)\int_{-\infty}^{x}(|a_1|^2 + |a_2|^2)dx']$, $a_2^* = \tilde{a}_2^* \exp[-i(T/v)\int_{-\infty}^{x}(|a_1|^2 + |a_2|^2)dx']$, it is possible to get an equation for $\tilde{a}_1$, $\tilde{a}_2$ in the form similar to Eq. (2) but with $\tilde{T} = 0$ and $\tilde{S} = S - T/2$. This new equation is invariant with respect to the substitution $\tilde{a}'\sqrt{\tilde{S}'} = \tilde{a}\sqrt{\tilde{S}}$, i.e., the coefficient $\tilde{S}$ only defines the amplitude scale, while the solution remains the same (except in the case $\tilde{S} \to 0$, when the currently ignored higher-order nonlinear interaction terms should be taken into account).

The transmission characteristics, calculated from the numerical solution of Eq. (2), are shown in Fig. 2. It is clear that they almost perfectly match the results of the previously performed micromagnetic simulations but with the coefficient $\tilde{S}$ that is different from the analytically calculated one. The nonlinear coefficients calculated using Ref. 31 are $T/(2\pi) = -8.06$ GHz and $S/(2\pi) = -1.46$ GHz, resulting in $\tilde{S}/(2\pi) = 2.57$ GHz, while the good agreement with the micromagnetic results is achieved for $\tilde{S}/(2\pi) \approx 4.75$ GHz (85% higher value). We believe that this discrepancy is mainly related to the influence of the nonresonant 3-wave interaction processes between different SW branches, which leads to the renormalization of the 4-magnon coefficients T and S. Note that these 3-magnon processes do not result in any qualitative difference but only in a weak quantitative difference.

Using the analytical model Eq. (2), it is possible to investigate how the transmission characteristics change with the size variation of the amplification gate. The pumping strength for each gate size L_a was chosen in such a way that the amplification rate in the linear regime is the same. As one can see from Fig. 3(a), the nonlinear processes, resulting in a decrease in the amplification efficiency, become pronounced at a smaller amplitude of the incident SW for longer amplification gates. Such a behavior is expected, as the strength of the nonlinear SW interaction depends on the amplitudes of both the incident and idler SWs. In the case of a smaller gate, the idler wave reaches a smaller amplitude

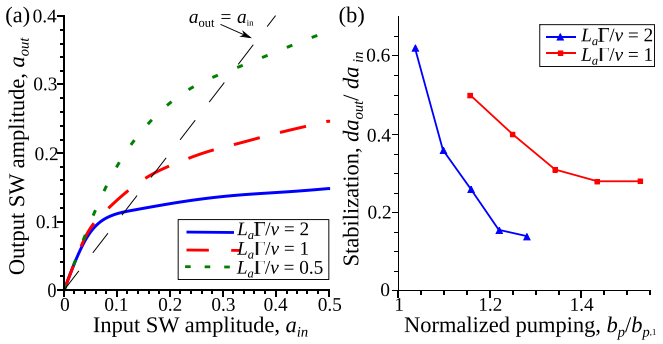

FIG. 3. (a) Transmission characteristics of the parametric amplifier calculated from the numerical solution of Eq. (2) for different lengths of the pumping localization region; (b) Stabilization ratio defined as a derivative da_{out}/da_{in} at the point $a_{out} = a_{in}$ for different pumping localization lengths. The pumping strength was normalized to the value $b_{p,1}$ at which $K = 1$ in the linear regime.

(remember that $a_2(x_C) = 0$), and the overall efficiency of the 4-wave interaction is also smaller. Thus, for the purpose of the SW amplification, it is desirable to use relatively small amplification gates with a length that is at least several times smaller than the SW mean free path $l_{fp} = v/\Gamma$.

In contrast, a better stabilization of the SW amplitude is achieved for larger gates having the size of the order or larger than the SW mean free path. The better stabilization properties correspond to a smaller derivative of the transmission characteristic at the point $a_{out} = a_{in}$. As one can see from Fig. 3(b), this amplitude stabilization effect is realized for a larger length of the pumping localization region and a higher pumping amplitude. Of course, the pumping amplitude should be smaller than the threshold of parametric excitation of SWs. For example, for $L_a\Gamma/v = 2$, the minimum value of the derivative da_{out}/da_{in} is $da_{out}/da_{in} \approx 0.13$, meaning that the amplitude spread in the output SW is 7.7 times smaller than the amplitude spread of the input SWs. Of course, in practical devices, the use of such large amplification gates is not convenient. A possible solution to this problem is a local variation of the SW dispersion, e.g., by the application of a static electric field (in the VCMA devices), or a variation of the nanowire shape. This dispersion variation allows one to change locally the SW wave vector and, therefore, the SW group velocity to satisfy the relation $v < L_a\Gamma$, while the SW mean free path outside of this region can be substantially larger.

The model Eq. (2) also allows one to estimate the characteristic amplitudes of the incident SW at which different amplification regimes can be realized. In particular, a linear amplification regime is realized in the range of $|a_{in}|^2 \ll 1/(\tilde{S}\sqrt{\langle f^2(x)\rangle})$, where the function $f(x)$ is $f(x) = (K^2/v\kappa)\sin[\kappa(x_C - x)](\cos[\kappa(x_C - x)] + \Gamma/(v\kappa)\sin[\kappa(x_C - x)])$ and the symbol $\langle\ldots\rangle$ denotes the averaging over the pumping region. In contrast, a SW is almost insensitive to the pumping and simply decays as $\exp[-\Gamma x/v]$ in the range of $|a_{in}|^4 \gg v/(2\Gamma L_a)|Vb_p/\tilde{S}|^2 \exp[2\Gamma L_a/v]$. The results calculated from these expressions are in good agreement with the results of our numerical simulations. The details of the derivation can be found in the supplementary materials.

At the end, we would like to note that the nonlinear coefficients T_k and S_k could significantly depend on the nanowire geometry and the static magnetization as well as on the SW wave vector k. Thus, by choosing a proper geometry and a proper working frequency, it is possible to both enhance and suppress the nonlinear interactions at a given SW amplitude, depending on what is desired.

In summary, we have studied a nonlinear stage of amplification of a propagating SW by a localized parametric pumping. It was shown that the nonlinear 4-wave interaction processes result in the decrease in a parametric amplification efficiency at sufficiently high SW amplitudes. The characteristic values of the SW amplitudes, at which the nonlinear interaction becomes important, are determined by 4-wave interaction efficiency (coefficient $\tilde{S}$) and are inversely proportional to the ratio of the pumping localization length L_a to the SW mean free path l_{fp}. As a result, for the purpose of the SW amplification, it is desirable to use relatively small amplification gates, which can efficiently amplify large-amplitude SWs. In contrast, larger gates ($L_a \gtrsim l_{fp}$) with the pumping strength that is close to the parametric excitation threshold can be used for the stabilization of the SW amplitude.

See supplementary materials for the details of the estimation of SW amplitudes at which different regimes of the parametric amplification are realized.

This work was supported in part by the grant from the Center for NanoFerroic Devices (CNFD) and Nanoelectronics Research Initiative (NRI), by the Grants Nos. EFMA-1641989 and ECCS-1708982 from the NSF of the USA, and by the DARPA M3IC Grant under the Contract No. W911-17-C-0031. RV acknowledges support from the Ministry of Education and Science of Ukraine, project 0115U002716. G.F. and M.C. acknowledge the executive program of scientific and technological cooperation between Italy and China for the years 2016–2018 "Nanoscale broadband spin-transfer-torque microwave detector" (code CN16GR09) funded by Ministero degli Affari Esteri e della Cooperazione Internazionale.

[1]A. Khitun, M. Bao, and K. L. Wang, J. Phys. D: Appl. Phys. **43**, 264005 (2010).
[2]A. V. Chumak, V. I. Vasyuchka, A. A. Serga, and B. Hillebrands, Nat. Phys. **11**, 453 (2015).
[3]A. V. Chumak, A. A. Serga, and B. Hillebrands, Nat. Commun. **5**, 4700 (2014).
[4]V. V. Kruglyak, S. O. Demokritov, and D. Grundler, J. Phys. D: Appl. Phys. **43**, 264001 (2010).
[5]T. Schneider, A. A. Serga, B. Leven, B. Hillebrands, R. L. Stamps, and M. P. Kostylev, Appl. Phys. Lett. **92**, 022505 (2008).
[6]N. Sato, K. Sekiguchi, and Y. Nozaki, Appl. Phys. Express **6**, 063001 (2013).
[7]R. L. Melcher, Phys. Rev. Lett. **30**, 125 (1973).
[8]L. Udvardi and L. Szunyogh, Phys. Rev. Lett. **102**, 207204 (2009).
[9]V. L. Zhang, K. Di, H. S. Lim, S. C. Ng, M. H. Kuok, J. Yu, J. Yoon, X. Qiu, and H. Yang, Appl. Phys. Lett. **107**, 022402 (2015).
[10]M. Weisheit, S. Fähler, A. Marty, Y. Souche, C. Poinsignon, and D. Givord, Science **315**, 349 (2007).
[11]C.-G. Duan, J. P. Velev, R. F. Sabirianov, Z. Zhu, J. Chu, S. S. Jaswal, and E. Y. Tsymbal, Phys. Rev. Lett. **101**, 137201 (2008).
[12]J. Zhu, J. A. Katine, G. E. Rowlands, Y.-J. Chen, Z. Duan, J. G. Alzate, P. Upadhyaya, J. Langer, P. K. Amiri, K. L. Wang, and I. N. Krivorotov, Phys. Rev. Lett. **108**, 197203 (2012).
[13]K. Nawaoka, Y. Shiota, S. Miwa, H. Tomita, E. Tamura, N. Mizuochi, T. Shinjo, and Y. Suzuki, J. Appl. Phys. **117**, 17A905 (2015).

[14]Y.-J. Chen, H. K. Lee, R. Verba, J. A. Katine, I. Barsukov, V. Tiberkevich, J. Q. Xiao, A. N. Slavin, and I. N. Krivorotov, Nano Lett. **17**, 572 (2017).
[15]B. Rana, Y. Fukuma, K. Miura, H. Takahashi, and Y. Otani, Appl. Phys. Lett. **111**, 052404 (2017).
[16]K.-S. Lee and S.-K. Kim, J. Appl. Phys. **104**, 053909 (2008).
[17]S. Klingler, P. Pirro, T. Brächer, B. Leven, B. Hillebrands, and A. V. Chumak, Appl. Phys. Lett. **105**, 152410 (2014).
[18]V. S. L'vov, *Wave Turbulence under Parametric Excitation* (Springer-Verlag, New York, 1994).
[19]B. Kalinikos, N. Kovshikov, M. Kostylev, and H. Benner, JETP Lett. **64**, 171 (1996).
[20]B. A. Kalinikos and M. P. Kostylev, IEEE Trans. Mag. **33**, 3445 (1997).
[21]P. A. Kolodin, P. Kabos, C. E. Patton, B. A. Kalinikos, N. G. Kovshikov, and M. P. Kostylev, Phys. Rev. Lett. **80**, 1976 (1998).
[22]T. Brächer, P. Pirro, and B. Hillebrands, Phys. Rep. **699**, 1 (2017).
[23]R. Verba, M. Carpentieri, G. Finocchio, V. Tiberkevich, and A. Slavin, Sci. Rep. **6**, 25018 (2016).
[24]R. Verba, M. Carpentieri, G. Finocchio, V. Tiberkevich, and A. Slavin, Phys. Rev. Appl. **7**, 064023 (2017).
[25]A. G. Gurevich and G. A. Melkov, *Magnetization Oscillations and Waves* (CRC Press, New York, 1996), p. 464.
[26]G. A. Melkov, A. A. Serga, V. S. Tiberkevich, Y. V. Kobljanskij, and A. N. Slavin, Phys. Rev. E **63**, 066607 (2001).
[27]A. A. Serga, S. O. Demokritov, B. Hillebrands, S.-G. Min, and A. N. Slavin, J. Appl. Phys. **93**, 8585 (2003).
[28]T. Brächer, F. Heussner, P. Pirro, T. Meyer, T. Fischer, M. Geilen, B. Heinz, B. Lägel, A. A. Serga, and B. Hillebrands, Sci. Rep. **6**, 38235 (2016).
[29]L. Lopez-Diaz, D. Aurelio, L. Torres, E. Martinez, M. A. Hernandez-Lopez, J. Gomez, O. Alejos, M. Carpentieri, G. Finocchio, and G. Consolo, J. Phys. D: Appl. Phys. **45**, 323001 (2012).
[30]V. Puliafito, A. Giordano, A. Laudani, F. Garescì, M. Carpentieri, B. Azzerboni, and G. Finocchio, Appl. Phys. Lett. **109**, 202402 (2016).
[31]P. Krivosik and C. E. Patton, Phys. Rev. B **82**, 184428 (2010).